Supplementary Information

Nearly total optical transmission of linearly polarised light through one-dimensional gold grating assisted by monolithic high-contrast grating

Landobasa Y. M. Tobing[1], Michał Wasiak[2], Dao Hua Zhang [1*], Weijun Fan[1*] and Tomasz Czyszanowski[2*]

[1]School of Electrical & Electronic Engineering, Nanyang Technological University, 50 Nanyang Avenue, Singapore, 639798

[2] Photonics Group, Institute of Physics, Łódź University of Technology, ul. Wolczanska 219, 90-924 Łódź, Poland

This PDF file includes:

Supporting information S1 and S2

Figs. S1 to S4

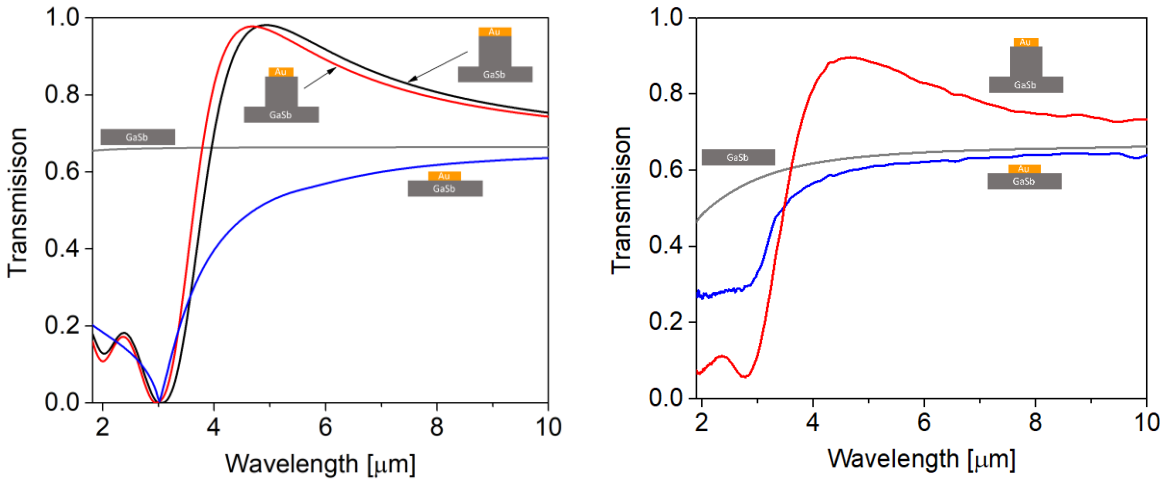

Fig. S1 Calculated a) and measured b) spectra of transmittance of metalMHCG for TM polarisation in the case of the structure with equal width of gold and semiconductor stripes (black) and narrower gold stripe with respect to semiconductor stripe as in the experiment (red). Blue curve represents grating of the same L, a, H_m as metalMHCG but with $H = 0$ that represents metal stripes deposited on the plane GaSb layer. Grey line represents Fresnel transmission through plane interface between GaSb and air. The discrepancy between theoretical and experimental curves in the range of short wavelengths originates from the tail of interband absorption in the GaSb. Parameters used in calculations: $L = 0.793$ μm, $a = 0.509$ μm, $H = 0.397$ μm , $H_m = 0.050$ μm. The width of the narrower gold stripes $a_m = 0.427$ μm (black and blue curves).

Supplementary S1: Device fabrication

The GaSb-Au hybrid structures were realized by combinations of electron beam lithography (EBL) patterning and dry etching in the fabrication steps illustrated in Fig. S2. The GaSb substrate was first spin coated with 250-nm thick ZEP520A-7 *e*-beam resist, followed by EBL patterning (20 keV beam energy, ~130 pA beam current, ~50-60 μC/cm^2 exposure dose), and cold development in methyl-isobuthyl ketone (MIBK) at 6°C for 35s. Gold grating structures were then realized by evaporating 50-nm thick Au (with 3 nm Ti as adhesion layer) and lift-off pattern transfer in warm *n*-methyl pyrrolidone (NMP) solution for 10-20 mins. Next, the sample was subjected to plasma-enhanced chemical-vapor deposition (PECVD) of 100-nm thick SiO_2, followed by a second EBL patterning (aligned with the first patterns), based on the same development process. The reactive ion etching (RIE) of SiO_2 was then conducted for hard mask definition, followed by ZEP520A resist removal in NMP solution. Afterwards, GaSb substrate was dry etched in inductively-coupled plasma RIE (ICP-RIE) system, using Cl_2/N_2 chemistry at 60°C temperature, 800W ICP power, 80W RF power, and ~110-120V DC bias. Finally, the device fabrication was finalized by removing the SiO_2 hard mask in hydrofluoric acid (HF) solution.

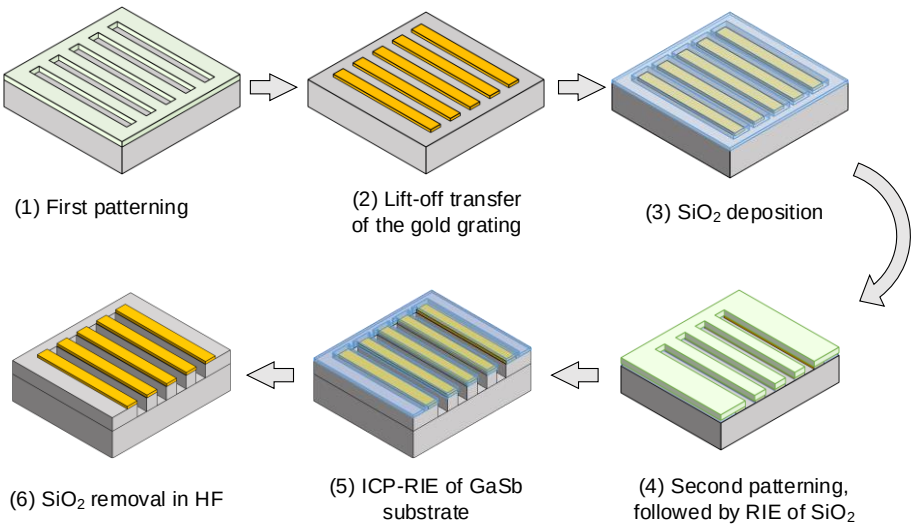

Figure S2. Fabrication steps of the GaSb-Au metalMHCG. (1) The first EBL patterning for the gold nanostructure, followed by cold development in MIBK for 35s. (2) Physical deposition of 50-nm thick gold, followed by lift-off in n-methyl pyrrolidone for 10 mins. (3) PECVD of 100 nm thick SiO_2. (4) Second EBL patterning for hard mask definition, followed by RIE of SiO2 and resist removal. (5) ICP-RIE of GaSb using Cl_2/N_2 chemistry. (6) SiO_2 removal in HF.

Supplementary S2: Measurements

The spectral characteristics of the fabricated GaSb-Au metalMHCG were locally measured in microscope system using mid-IR light sources from Fourier Transform Infrared Spectroscopy (FTIR, Vertex 70, Bruker Corp), and Mercury Cadmium Telluride (MCT) mid-IR photodetector (see Fig. S3). Prior to entering the microscope as the light source, the broadband light was first processed by the Michelson Interferometer in the FTIR system (using KBr beam splitter), which was then focused and collected by IR objective lens. For reflection measurement, the sample was illuminated from the top, and the reflected signals are collected by the IR objective lens (36x objective lens, reflection-type, NA = 0.5). The sizes of the top aperture were adjusted so as to only contain the devices (typically in 40µm x 40µm sizes). The reflected signals were normalized by the reflectance of a 50-nm thick Au film on the same GaSb substrate (collected through the same top aperture sizes). For transmission measurement, the light source comes from the bottom through an IR condenser under Kohler illumination. The bottom aperture was aligned with the top aperture, with their sizes adjusted to be slightly smaller than those of the top aperture. Afterwards, the microscope was turned into reflection mode to locate the devices before it was turned into transmission mode for transmission measurements. The transmitted signals from the nanostructures were normalized with the transmission spectra across the GaSb substrate. Different polarizations were introduced by adjusting the polarization slider at the top. The FTIR characterizations were conducted at 16 cm^{-1} resolution, averaged 64 times. The spectral noise for wavelength shorter than 2 µm is expected due to the ~1.7 µm bandgap of the GaSb.

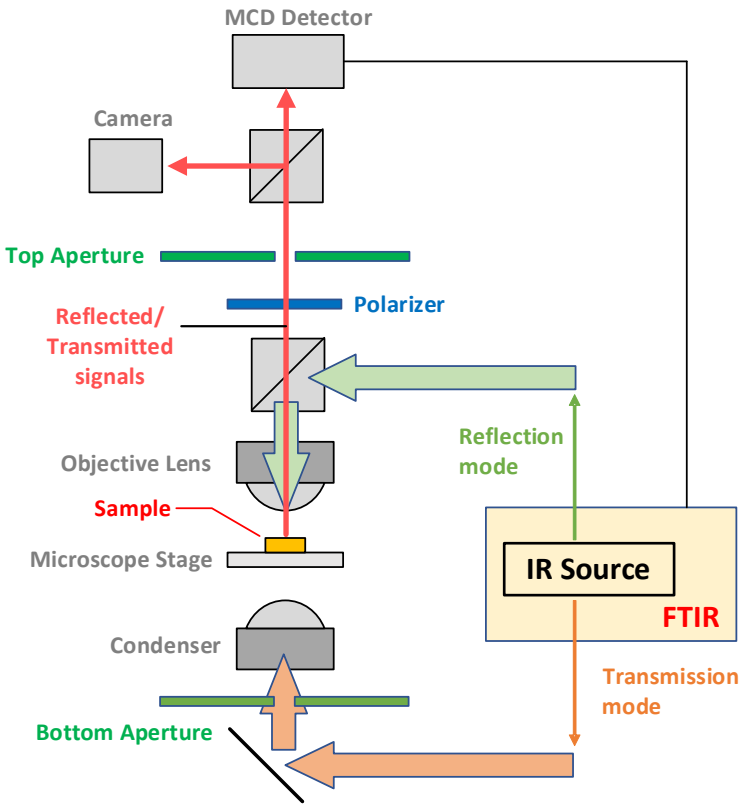

Fig. S3. Schematic for infrared transmission and reflection characterization of the GaSb-Au metalMHCG.

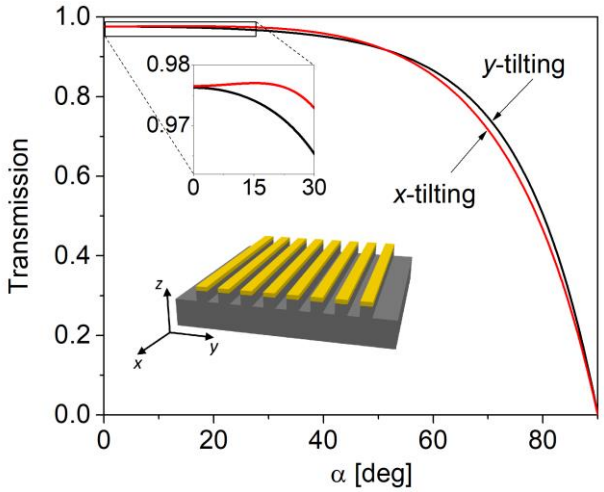

Fig. S4 Transmission of metalMHCG as the function of angle of incidence from the side of air. The parameters of the metalMHCG are as follows: L = 0.793 μm, a = 0.509 μm, H = 0.397 μm, H_m = 0.050 μm, a_m = 0.427 μm and wavelength of 4.64 μm.

Supplementary S3: Resistance Measurements

We characterize the device by the slope of the V-I characteristics. We first connect the device with two electrodes, using silver conductive paste (Ag paste), positioned by optical stages shown in Fig. S5a.

A drop of Ag paste is applied to the tip of the applicator (shown in Fig. S5b), followed by moving down the stage towards the sample. Upon nearly touching the surface of the sample, the applicator (or the sample) is moved so as to drag the paste to form an electrode. One example is presented in Fig. S5c, showing a device (of 100µm footprint) is successfully connected by two electrodes. Afterwards, the sample is subjected to a soft bake at 105°C for 4 mins to dry the Ag paste, where a simple resistance measurement across the Ag paste is used to ensure that the electrodes are already formed (with typical values of a few Ω). Afterwards, the device is characterized in terms of its V-I response, based on setup described in Fig. S6. The linear V-I characteristic from the probe measurement (Fig. S7) indicates ohmic contact, with the device resistance of R_{device} = 55.1 Ω extracted from the slope.

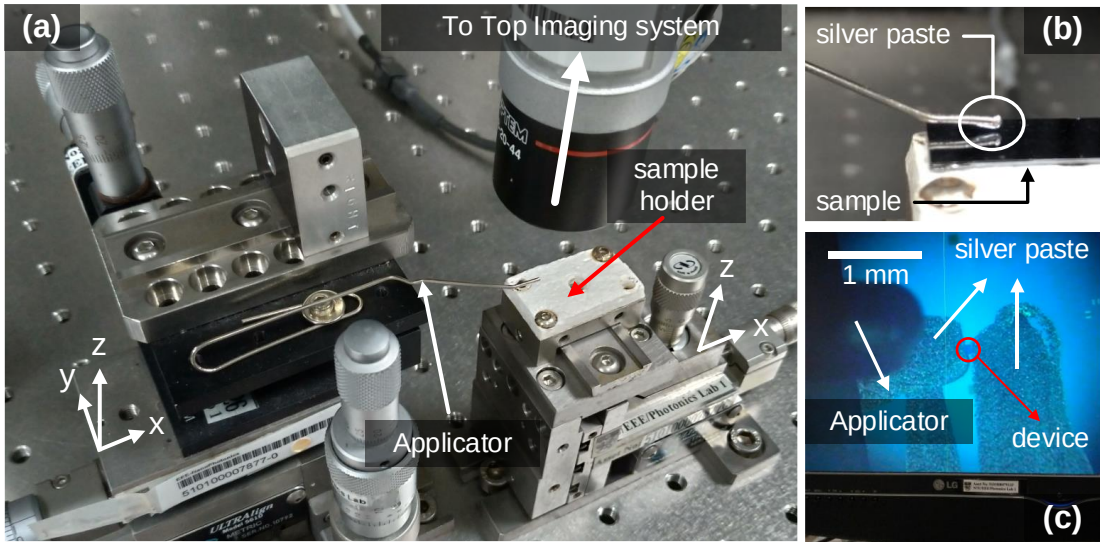

Fig. S5. (a-b) Customized applicator of silver conductive paste for local resistance measurement. (c) sample with silver paste applied onto device of 100µm footprint.

The relation between the resistance (R) and sheet resistance (R_s) is expressed as $R = R_s(L/W)$, where L (W) is the length (width) of the Au stripe. The current flow between the Ag paste electrodes occurs along the gold stripes that are not covered by the paste. Due to nonideal paste deposition the lengths of the stripes that are uncovered by the paste are different. We account their different lengths using the following formula to calculate the effective ratio of L/W:

$$\left(\frac{L}{W}\right)_{eff} = \left(W\sum_{i=1}^{n} L_i^{-1}\right)^{-1}$$

The lengths of the stripes are deduced from optical microscope image of the sample. The sheet resistance then is $R_s = R(W/L)_{eff} = 26.2 \pm 0.5\Omega\text{sq}^{-1}$ and resistivity of Au stripes is $\rho_{str} = 130 \times 10^{-8}\ \Omega\text{m}$.

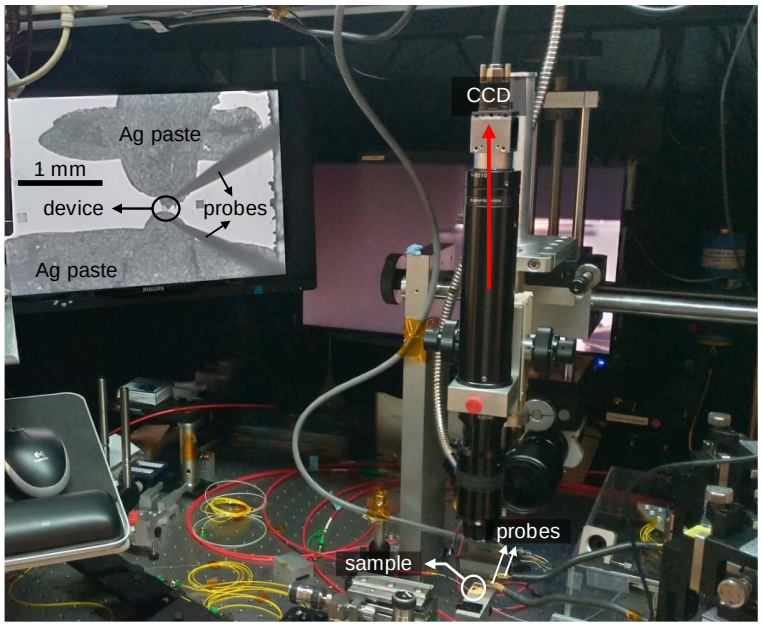

Fig. S6. Setup for V-I characterization

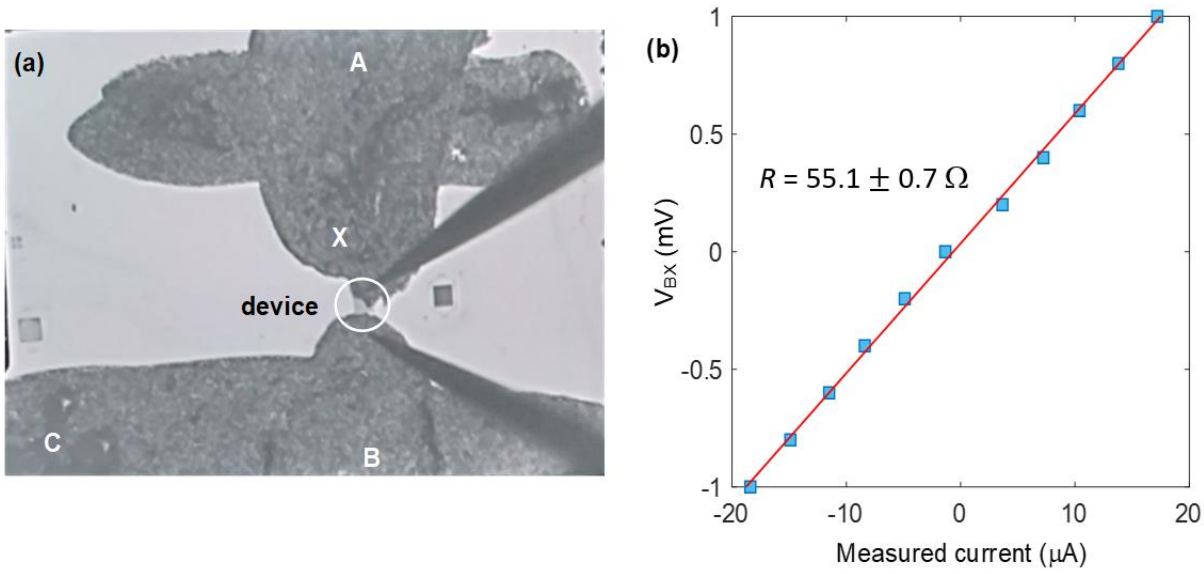

Fig. S7. (a) MetalMHCG structure connected with silver conductive paste. (b) V-I characteristics, showing device resistance of R_{device} = 55.1 Ω.

For the sake of validation of the above result we performed the measurement of sheet resistance of a gold 70 nm thick film on silicon substrate, which was physically deposited by the same e-beam evaporation process as in our device. The measured sheet resistance was found to be $R_s^{film} = 2.2\ \Omega\text{sq}^{-1}$, which indicates the resistivity of $\rho_{film} = 15.4 \times 10^{-8}\ \Omega\text{m}$ for a given film thickness. We found that this value is larger than that of the bulk gold, i.e. $\rho_{bulk} = 2.2 \times 10^{-8}\ \Omega\text{m}$, which is likely caused by the grain sizes and roughness of the physically deposited gold film. Based on our measurements the sheet resistance of the metalMHCG is found to be 12 times larger than that of the gold film.

We compare the measured resistivity with our previous numerical estimation based on bulk gold resistivity and its conductivity-size effects. The sheet resistance for the thin gold film calculated based on bulk gold resistivity is $R_s^{film} = 0.31\ \Omega\mathrm{sq}^{-1}$, while the sheet resistance of the device is numerically estimated as $R_s = 2.21 \pm 0.01\ \Omega\mathrm{sq}^{-1}$(from the manuscript). This suggests that the sheet resistance of the metalMHCG is ~7x higher than that of the thin film. This is consistent with our experimental values, where the sheet resistance of the metalMHCG was observed to be 12 times larger than that of the thin film. In addition to the grain boundaries of the gold thin film, we also believe that the sidewall roughness of the gold nanowires also contributes to increasing the gold resistivity.